Chinese Chemical Letters 37 (2026) 111614

Contents lists available at ScienceDirect

Chinese Chemical Letters

journal homepage: www.elsevier.com/locate/cclet

Flexible two-dimensional uranium-organic framework with upgraded radiation resistant for X-ray imaging

Jueqiong Wang[a,1], Liwei Cheng[a,1], Yang Yang[a], Dewen He[a], Yingtong Fan[a], Zhiwei Li[a], Junhao Lu[a], Yumin Wang[a], Jia Lei[a], Zhiyong Peng[a], Aiping Jin[c], Dan Zhou[a], Zhizai Li[a], Shuaihua Wang[b,*], Lixi Chen[a,*], Yaxing Wang[a], Yanlong Wang[a,*], Shuao Wang[a,*]

[a] State Key Laboratory of Radiation Medicine and Protection, School of Radiation Medicine and Protection, Collaborative Innovation Center of Radiological Medicine of Jiangsu Higher Education Institutions, Soochow University, Suzhou 215123, China
[b] Key Laboratory of Optoelectronic Materials Chemistry and Physics, Fujian Institute of Research on the Structure of Matter, Chinese Academy of Sciences, Fuzhou 350002, China
[c] CNNP Nuclear Power Operations Management Co., Ltd., Haiyan 314303, China

ARTICLE INFO

Article history:
Received 13 March 2025
Revised 27 June 2025
Accepted 19 July 2025
Available online 20 July 2025

Keywords:
Uranium
Metal-organic framework
X-ray excited luminescence
X-ray irradiation stability
X-ray imaging

ABSTRACT

The intrinsic scintillation property of uranium has recently endowed this heaviest naturally occurring element with new opportunities for X-ray radiation detection and visualization. However, the low radiation stability of most uranium compounds hinders their practical application, particularly in X-ray imaging. Here, we presented a flexible two-dimensional uranium-organic framework (UOF, SCU-334) as an air-stable scintillating material for X-ray detection and, for the first time, a systematic investigation of X-ray imaging in UOFs. Following continuous high dose rate X-ray irradiation exceeding 50 Gy, which equals thousands of chest X-ray diagnoses, SCU-334 retains over 90% of its initial performance, representing a significant improvement over previously reported scintillating UOFs. The upgraded radiation resistance of SCU-334 is attributed to its flexible structure that dissipates energy more efficiently under high-energy particle bombardment through conformation fluctuation and relaxation. This work offers a promising approach to improve the radiation resistance of uranium-based scintillators.

© 2026 Published by Elsevier B.V. on behalf of Chinese Chemical Society and Institute of Materia Medica, Chinese Academy of Medical Sciences.

X-ray imaging, renowned for its superior penetrating capabilities, finds extensive application including medical diagnostic imaging [1], radiation detection [2] and non-destructive testing (NDT) [3]. Scintillating materials play a crucial role in X-ray imaging [4–9]. By absorbing X-rays through photoelectric effect or Compton scattering, scintillators convert high energy X-ray into low-energy photons that can be detected by versatile detectors or, if within visible spectrum, directly visualized by camera [10,11]. Commercial scintillators can be classified into inorganic and organic scintillators [4,12–15]. Inorganic scintillators, such as CsI:Tl [16] and $Bi_4Ge_3O_{12}$ [17], were typically prepared under harsh conditions to yield densely packed structures. Although possessing high X-ray attenuation coefficient, inorganic scintillators also suffer significant damage from absorbed high energy radiation, which usually creates continuous defects [18] that can reduce their operational stability in atmospheric conditions for X-ray imaging. Organic scintillators [19], such as fluorene derivatives [20] and anthracene [1,21], can be prepared under mild conditions, but the lack of heavy elements results in lower X-ray absorptivity and sometimes poorer X-ray responsiveness [22,23], which may reduce the X-ray imaging resolution. Exploring novel imaging materials exhibiting excellent scintillating performance, radiation stability and facile preparation conditions is a major focus of the cutting-edge research.

Organic-inorganic hybrid materials, including metal-organic frameworks (MOFs) [18,21,24–27], perovskite [12,28,29], recently emerge as a promising category in radiation detection and imaging. The on-demand combination of inorganic and organic components enables the programmable regulation of their X-ray absorptivity and energy conversion efficiency [8,27,30–32]. Possessing both the naturally highest atomic mass (high Z_{eff}) and intrinsic luminescence, uranium has been recognized as an ideal building block for constructing organic-inorganic hybrid scintillators [33–35]. Our group has pioneered the exploration of uranium-based compounds as scintillators [36–41]. Logically, a trade-off issue remains between scintillating performance and radiation stability. On

* Corresponding authors.
E-mail addresses: shwang@fjirsm.ac.cn (S. Wang), lxchen@suda.edu.cn (L. Chen), ylwang@suda.edu.cn (Y. Wang), shuaowang@suda.edu.cn (S. Wang).
[1] These authors contributed equally to this work.

https://doi.org/10.1016/j.cclet.2025.111614
1001-8417/© 2026 Published by Elsevier B.V. on behalf of Chinese Chemical Society and Institute of Materia Medica, Chinese Academy of Medical Sciences.

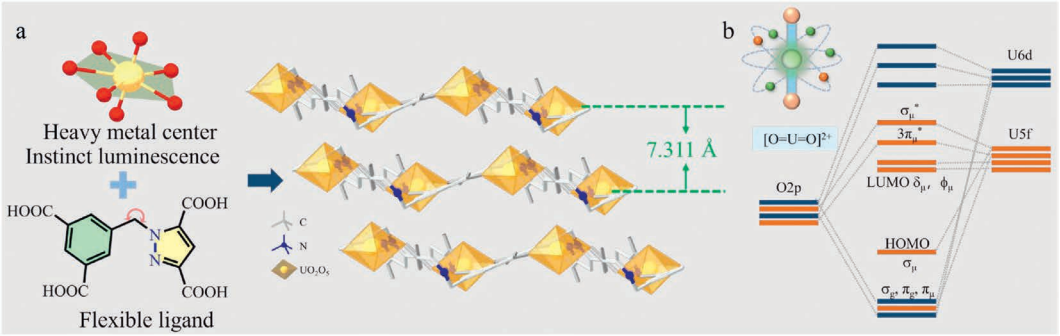


Fig. 1. (a) Structure of ligand for SCU-334 (left). A three-dimensional view of the stacking of the two-dimensional layers of the SCU-334 along the [101] plane (right). The N atom is shown in blue, the U is shown in yellow, the C is performed in gray, the U-O bond and H atom are hidden. (b) Schematic diagram of the valence orbitals of UO_2^{2+} (the 6p and 6s orbitals of uranium atom and 2s orbitals of oxygen atom are omitted, only orbitals participating in HOMO-LUMO are illustrated).

the one hand, the high Z_{eff} of uranium guarantees a higher interaction section between scintillators and incident high-energy rays, which benefits the sensitive response to a low dose X-ray irradiation. On the other, the absorbed X-ray, whose energy is far beyond any chemical bonds, severely damages the crystalline structure, leading to poor radiation resistance under accumulated irradiation. For instance, the first U-based scintillator, SCU-9, retained only 65 % of its original XEL intensity after 53 Gy of X-ray irradiation [36]. The first uranium-based inorganic scintillator, UMO, maintained 75 % XEL performance after the same radiation dose [37]. The first uranyl molecular cluster shows better radiation stability, which also suffers >10 % of its XEL intensity after 40 Gy [42]. To date, only one uranium-based scintillator, U-pba, has shown relatively better radiation stability, which benefits the preliminary X-ray imaging exploration, albeit with low resolution [38]. As a result, there remains substantial scope for further enhancing the radiation stability of uranium-based scintillators and, more importantly, for improving the quality of X-ray imaging.

Herein, we presented a flexible two-dimensional uranium-organic framework (UOF, SCU-334) containing dense hydrogen bonds for X-ray scintillation and imaging. The broad interlayer distance (>7 Å) and the flexible linker (1-(3,5-dicarboxybenzyl)-1*H*-pyrazole-3,5-dicarboxylic acid, H_4L) (Fig. 1a) enables energy absorption and dissipation through conformational adaptation and structural relaxation when bombarded by high energy particles. Moreover, the abundant hydrogen bonds in SCU-334 facilitate radical scavenging and self-healing, ensuring structural integrity upon radiation exposure. All these features contribute to upgraded radiation stability for X-ray imagining.

The solvothermal reaction of uranyl nitrate hexahydrate, H_4L, acetonitrile (CH_3CN), nitric acid, and deionized water yields pure yellow crystals of a two-dimensional layered uranium MOF, $[(UO_2^{2+})(H_2L^{2-})]\cdot CH_3CN\cdot 2(NH_3)\cdot 6H_2O$, abbreviated as SCU-334 (Fig. 1a). Single-crystal X-ray diffraction (SC-XRD) analysis reveals that SCU-334 crystallizes in the triclinic space group *P*-1 (structure refinement details in Table S1 in Supporting information, CCDC No. 2410527). The asymmetric unit of SCU-334 consists of one UO_2^{2+} ion, one H_2L^{2-} ligand, and one free H_2O molecule linked by hydrogen bonds (Fig. S1 in Supporting information). Each UO_2^{2+} metal center is coordinated to five oxygen atoms from four adjacent ligands, forming a pentagonal bipyramidal geometry (Fig. S1a). Meanwhile, each ligand binds to four surrounding UO_2^{2+} cations, further creating a two-dimensional layer with *sql* topology. As shown in Fig. S1d, the carboxyl groups of the H_2L^{2-} ligand are not fully coordinated to the UO_2^{2+} ions, resulting in three uncoordinated oxygen atoms (Fig. S1e). As illustrated in Fig. 1a, the 2D layers are stacking along the [101] plane with an average interlayer distance of 7.311 Å. Notably, two types of hydrogen bonds are formed between the water molecules and ligands, one is O···H–O, and the other is N···H–O (Fig. S1c). The flexible linker and the rich hydrogen bonds endow SCU-334 with more flexibility than those MOFs constructed by rigid linker and strong coordination bonds. Overall, the crystal structure of SCU-334 could be described as a series of equatorial plane 5-coordination UO_2^{2+} linked by L^{4-} and H_2O. The densely packed fashion endows SCU-334 with relatively high X-ray attenuation efficiency (Fig. S2 and Table S2 in Supporting information). Although CsI:Tl and SCU-9 showed higher X-ray blocking ability, their relatively poorer X-ray stability may affect their long-term use under ambient conditions. The formula of SCU-334 is determined by element analysis (EA) and thermogravimetric analysis (TGA) (Fig. S3 in Supporting information). The phase purity of SCU-334 was confirmed by powder X-ray diffraction (PXRD) (Fig. S4 in Supporting information), while further compositional details were characterized by Fourier transform infrared spectroscopy (FTIR) and UV–vis absorption spectrum (Figs. S5 and S6 in Supporting information). The luminescence property of SCU-334 was investigated under excitation at 345 nm. As shown in Fig. S7 (Supporting information), the SCU-334 powder displays bright green luminescence. The emission spectrum reveals a quintet of peaks at 493, 513, 536, 561, and 588 nm, aligning with the characteristic signature of UO_2^{2+} luminescence spectra (Fig. S8 in Supporting information). Moreover, SCU-334 exhibits moderate fluorescence lifetime ($\tau = 67.2$ μs, Fig. S9 in Supporting information) [49] and relatively high photoluminescence quantum yield (19.34 %, Fig. S10 in Supporting information), which is higher than many carboxylate-based uranyl complexes (0.6 %–13 %) [38], indicating smooth energy transfer from ligand to uranyl and relatively lower non-radiative relaxation during transfer. The photothermal conversion efficiency of SCU-334 upon high flux radiation under Xe lamp was compared to SCU-9 (Figs. S11 and S12, Table S3 in Supporting information), which is a more rigid 2D UOF showing good X-ray excited luminescence (XEL). The infrared thermal images show a lower temperature increase for SCU-334 than SCU-9 (Fig. S13 in Supporting information), which suggests the potential role of flexible ligand to dissipate energy through the rich hydrogen bonds where high-frequency oscillator (O–H) was involved.

X-ray induced radioluminescence (RL) of SCU-334 was recorded using a spectrometer embedded within a laboratory X-ray source. Notably, the peak position and shape of the RL spectrum is perfectly parallel to that of the PL spectrum (Fig. S14 in Supporting information), suggesting similar emission pathways [36,50]: Similar to excitation by ultraviolet light, when the luminescent center UO_2^{2+} in the MOF absorbs X-ray energy exceeding the threshold required for electron transition, the ground state electrons were excited to higher electronic energy level. These excited electrons deactivate spontaneously back to the ground state, during which

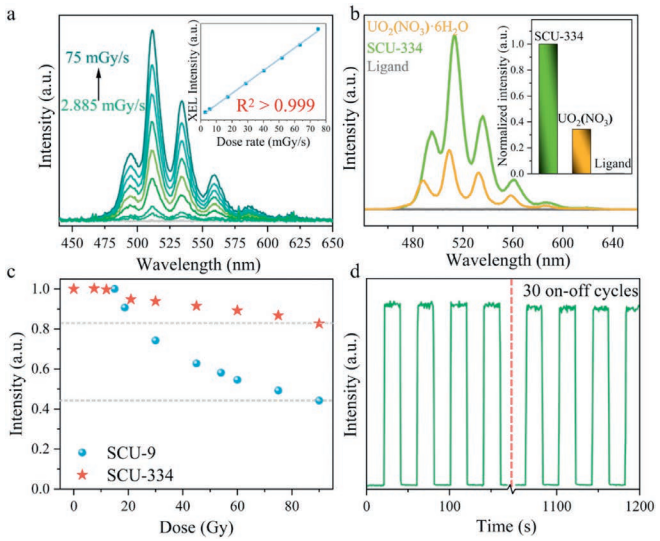


Fig. 2. (a) The XEL spectra of SCU-334 under X-ray irradiation of various X-ray power. Inset is the normalized XEL intensity at 513 nm *versus* X-ray flux intensity for SCU-334; the slope is relevant to the sensitivity of X-ray scintillators. (b) The normalized XEL intensity of SCU-334, $UO_2(NO_3)_2{\cdot}6H_2O$, and H_4L under the same experimental conditions. The Inset is the bar chart after the XEL strength has been normalized. (c) Normalized comparison of the initial XEL intensity of SCU-334 and SCU-9 with increasing X-ray irradiation dose of 90 Gy. (d) Reusability of the SCU-334. Each cycle received a 50 kV, 70 μA X-ray irradiation, and a total of 30 on-off cycles were repeated (40 s/cycle).

the UO_2^{2+} emits luminescence *via* a ligand-to-metal charge transfer (LMCT) process. The luminescence process involves the transfer of an electron from the 2p orbitals of the bound oxygen (σ_μ, σ_g, π_μ, π_g) to the non-bonding uranium 5f orbitals δ_μ and ϕ_μ (Fig. 1b). This unique property enables UO_2^{2+} to emit bright green light when stimulated by high-energy radiation, even in the absence of antenna ligands.

Dose-dependent RL intensity (2.885 mGy/s to 75 mGy/s), showed good linearity ($R^2 = 0.999$). Based on the fitted slope, the calculated detection limit (LOD) of SCU-334 is 325.81 μGy/s (Fig. 2a), indicating decent scintillation performance. The light yield of SCU-334 is 4363 photons/MeV (Fig. S15 in Supporting information), and no afterglow (Fig. S16 in Supporting information). To deeply evaluate the significance of constructing such organic-inorganic hybrid systems, the XEL signals of the precursors (H_4L and $UO_2(NO_3)_2{\cdot}6H_2O$) and the synthesized material (SCU-334) were compared at a fixed dose rate of 42.3 mGy/s (Fig. 2b), following the method in references [43,44]. The XEL intensity of SCU-334 materials outperformed those of uranyl nitrate salt and H_4L. This result demonstrates the significance of constructing MOF architecture for enhancing the performance of raw materials. Furthermore, radiation stability is a critical index to evaluate the practical performance of scintillators. PXRD and FT-IR results demonstrate that SCU-334 shows good stability in air and after 100 kGy γ-ray irradiation (Figs. S17 and S18 in Supporting information). The SCU-334 holds excellent XEL performance within 50 Gy (<10% drop in intensity), which equals 5000–10,000 times chest X-ray diagnoses (~5–10 mSv per shoot, 1 mGy absorbed dose almost equals 1 mSv for human body). Even after continuous exposure of 90 Gy X-ray irradiation, the RL intensity remains over 80% of its initial luminescence (Fig. 2c). In sharp contrast, the RL intensity of SCU-9 constructed by uranyl and rigid ligand drops to <60% after 50 Gy and to ~40% after 90 Gy. The decent radiation stability of SCU-334 is attributed to the flexible structure and rich hydrogen bonds within the SCU-334. Electron paramagnetic resonance (EPR) verified that X-ray irradiation produced a significant number of radicals (Fig. S19 in Supporting information), which may lead to bond cleavage and performance degradation. It has been reported that abundant hydrogen bonds can capture and passivate radiation-induced radicals [45]. Single-crystal structure analysis reveals that SCU-334 contains an extensive hydrogen-bonding network (four hydrogen bonds exist in the asymmetric unit containing only one uranyl ion, Fig. S1 in Supporting information). Compared to coordination and covalent bonds, hydrogen bonds, owing to their relatively weaker strength, may act as sacrificial bonds under irradiation to protect the structural integrity of SCU-334. Additionally, the reversible nature of hydrogen bonds facilitates self-healing after localized or minor structural damage [47], which may further enhance the material radiation resistance. In addition, the relatively flexible framework of SCU-334 also enhances radiation resistance by allowing atom/bond rearrangement after radiation damage [46–48]. PXRD and IR spectra analyses conducted before and after irradiation revealed no detectable structural changes for SCU-334 (Figs. S17 and S18). Notably, no significant decrease in XEL was observed after 30 on-off cycles (Fig. 2d). The environmental stability of a scintillator is crucial for its practical application. Results from varying humidity, temperature and long-term air exposure verified the superior operational stability of SCU-334 over commercial CsI:Tl (Figs. S20–S22 in Supporting information), highlighting the potential for long-term utility.

The excellent XEL and radiation resistance property of SCU-334 makes it promising for X-ray imaging. A flexible composite film was made through physical mixing of SCU-334 microcrystals with transparent polydimethylsiloxane (PDMS) matrix. The as-prepared 6.1 cm × 2.8 cm × 0.13 mm film was uniform (Fig. S23 in Supporting information) and exhibited flexible and bendable features (Fig. 3a). A target object was placed between the X-ray source and the SCU-334 thin-film screen, and the image was recorded by a digital camera (Fig. 3b). The MOF-based flexible X-ray detector exhibits an excellent spatial image resolution of approximately 11 line-pairs per millimeter (lp/mm) (Fig. 3c) validated by the modulation transfer function (MTF) data (Fig. S24 in Supporting information), which is comparable to that of conventional flat panel X-ray detectors and much better than the 4 lp/mm of the previously reported U-based scintillating film [38]. The as-prepared scintillator film successfully imaged several inorganic objects such as a spring in a pen cap (Fig. 3d), a mouse receiver (Fig. 3e), an earphone (Fig. S25 in Supporting information), a ballpoint pen (Fig. S25), and a dried specimen of an organic living fish (Fig. S25), further demonstrating its X-ray imaging capabilities. All these results corroborate the excellent imaging performance of the SCU-334 film. To verify the long-term stability of the SCU-334 scintillator film, a used film that had been stored for two months was tested again, as shown in Fig. S25. The imaging results demonstrated excellent clarity with no significant vagueness compared to the imaging quality of a freshly prepared film. Subsequently, we further evaluated the mechanical durability of the scintillator film. A newly fabricated film was bent for 200 cycles using a self-made apparatus (Figs. S26 and S27 in Supporting information). The imaging results revealed no noticeable change in imaging quality, confirming the excellent mechanical durability of the SCU-334 scintillator film. In addition, the potential scalability of large imaging devices is achieved by making scintillator films in larger sizes. As depicted in Fig. S28 (Supporting information), SCU-334 can be used in the same way to produce a larger film maintained the original fluorescence properties, which indicates the potential scalability of scintillator materials and scintillator films in large devices.

In summary, a novel two-dimensional flexible uranium-organic framework, SCU-334, was synthesized *via* solvothermal method, which exhibits bright green emission visible to the naked eyes under UV or X-ray irradiation. The flexible ligand strategy confers enhanced radiation stability for repeated use, paving the foundation

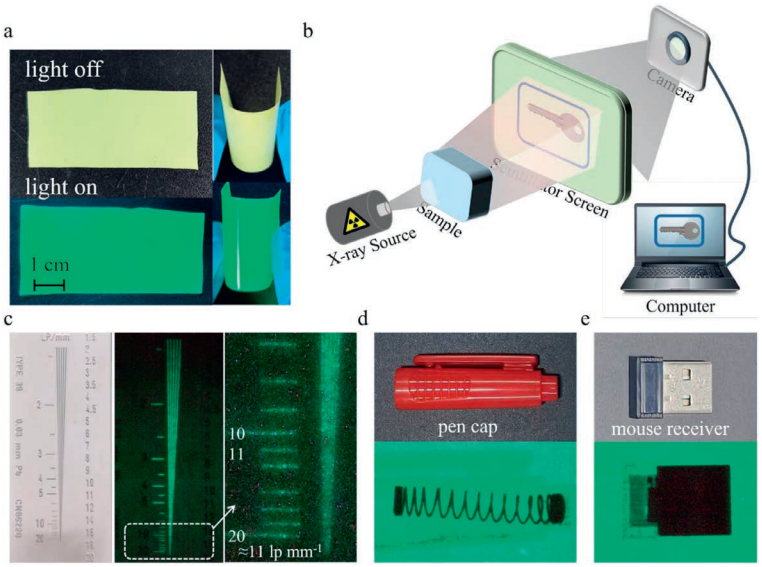


Fig. 3. (a) The photograph of a scintillator flexible film (*ca.* 6.1 cm × 2.8 cm × 0.13 mm) prepared for imaging. (b) A simple illustration of the built imaging device. (c) An image of the standard line-pair card of SCU-334. (d, e) Images of a spring inside the pen cap and a mouse receiver. The upper pictures are physical objects, and the bottom ones are X-ray imaging.

for X-ray imaging. A flexible membrane fabricated from SCU-334 microcrystals achieved the highest X-ray imaging resolution among yet reported uranium-based materials. This study expands the application of UOFs in the field of scintillators and proposes a new direction for the application of uranium-based hybrid materials.

Declaration of competing interest

The authors declare that they have no known competing financial interests or personal relationships that could have appeared to influence the work reported in this paper.

CRediT authorship contribution statement

Jueqiong Wang: Writing – review & editing, Writing – original draft, Validation, Methodology, Investigation, Funding acquisition, Formal analysis, Data curation, Conceptualization. **Liwei Cheng:** Writing – review & editing, Visualization, Supervision, Methodology, Funding acquisition, Data curation. **Yang Yang:** Formal analysis, Data curation. **Dewen He:** Supervision, Formal analysis. **Yingtong Fan:** Visualization, Data curation. **Zhiwei Li:** Software, Formal analysis. **Junhao Lu:** Methodology, Data curation. **Yumin Wang:** Supervision, Software, Resources. **Jia Lei:** Data curation. **Zhiyong Peng:** Supervision, Formal analysis. **Aiping Jin:** Funding acquisition. **Dan Zhou:** Writing – review & editing. **Zhizai Li:** Supervision, Data curation. **Shuaihua Wang:** Methodology, Formal analysis, Data curation. **Lixi Chen:** Writing – review & editing, Supervision, Resources, Project administration, Funding acquisition, Formal analysis, Conceptualization. **Yaxing Wang:** Supervision, Software, Methodology. **Yanlong Wang:** Supervision, Software, Resources, Project administration, Investigation, Funding acquisition, Conceptualization. **Shuao Wang:** Validation, Supervision, Project administration, Funding acquisition.

Acknowledgments

We are grateful for the financial support from the National Natural Science Foundation of China (Nos. 22376153, U23A20104, 22206144, 22276132, 22306139, 22076131). We also appreciate Science Foundation of the Higher Education Institutions of Jiangsu Province (No. 22KJA150006), Gusu Innovation and Entrepreneurship Leading Talent Program Project (No. ZXL2024406), Suzhou Fundamental Research Project (No. SJC2023001) and a Project Funded by the Priority Academic Program Development of Jiangsu Higher Education Institutions (PAPD).

Supplementary materials

Supplementary material associated with this article can be found, in the online version, at doi:10.1016/j.cclet.2025.111614.

References

[1] J. Perego, I. Villa, A. Pedrini, et al., Nat. Photonics 15 (2021) 393–400.
[2] R. Idoeta, M. Herranz, N. Alegría, F. Legarda, Appl. Radiat. Isot. 176 (2021) 109881.
[3] Q. Zhou, J. Ren, J. Xiao, et al., Nanoscale 13 (2021) 19894–19902.
[4] J.X. Wang, O. Shekhah, O.M. Bakr, M. Eddaoudi, O.F. Mohammed, Chem 11 (2024) 102273.
[5] J.X. Wang, O.M. Bakr, O.F. Mohammed, Matter 5 (2022) 2547–2549.
[6] Y. Wang, M. Li, Z. Chai, Y. Wang, S. Wang, Angew. Chem. Int. Ed. 62 (2023) e202304638.
[7] T. Wang, S. Hu, T. Ji, et al., Laser Photonics Rev. 18 (2024) 2300892.
[8] X. Zhang, H. Qiu, W. Luo, et al., Adv. Sci. 10 (2023) 2207004.
[9] A. Luo, J. Zhang, D. Xiao, et al., Nat. Commun. 15 (2024) 8181.
[10] M. Ghelman, N. Kopeika, S. Rotman, et al., IEEE T. Nucl. Sci. 71 (2024) 1072–1083.
[11] G. De Ninno, J. Wätzel, P.R. Ribič, et al., Nat. Photonics 14 (2020) 554–558.
[12] Q. Chen, J. Wu, X. Ou, et al., Nature 561 (2018) 88–93.
[13] T. Yanagida, P. Jpn. Acad. B: Phys. 94 (2018) 75–97.
[14] T. Martin, A. Koch, M. Nikl, MRS Bull. 42 (2017) 451–457.
[15] H. Wang, C. Peng, M. Chen, et al., Angew. Chem. Int. Ed. 63 (2024) e202316190.
[16] R. Hawrami, E. Ariesanti, A. Farsoni, et al., Crystals 12 (2022) 1517.
[17] A. Nassalski, M. Moszynski, A. Syntfeld-Kazuch, et al., IEEE T. Nucl. Sci. 55 (2008) 1069–1072.
[18] J.J. Perry Iv, P.L. Feng, S.T. Meek, et al., J. Mater. Chem. 22 (2012) 10235–10248.
[19] X. Ou, Z. Hong, Q. Wu, et al., ACS Nano 18 (2024) 27126–27137.
[20] Z. Han, H. Yu, Q. Pei, ACS Appl. Polym. Mater. 4 (2022) 4424–4431.
[21] C. Wang, O. Volotskova, K. Lu, et al., J. Am. Chem. Soc. 136 (2014) 6171–6174.
[22] T.J. Hajagos, C. Liu, N.J. Cherepy, Q. Pei, Adv. Mater. 30 (2018) 1706956.
[23] A. Sato, M. Koshimizu, Y. Fujimoto, et al., Mater. Chem. Front. 6 (2022) 1470–1476.
[24] F.P. Doty, C.A. Bauer, A.J. Skulan, et al., Adv. Mater. Adv. Mater. 21 (2009) 95–101.
[25] J. Perego, C.X. Bezuidenhout, I. Villa, et al., Nat. Commun. 13 (2022) 3504.
[26] J.X. Wang, L. Gutiérrez-Arzaluz, X. Wang, et al., Matter 5 (2022) 253–265.
[27] M. Orfano, J. Perego, F. Cova, et al., Nat. Photonics 17 (2023) 672–678.
[28] F. Liu, R. Wu, J. Wei, et al., ACS Energy Lett. 7 (2022) 1066–1085.
[29] W. Zhang, H. Wang, Z. Chen, Y. Shao, Laser Photonics Rev. (2024) 2400470.

[30] Q.C. Peng, Y.B. Si, J.W. Yuan, et al., Angew. Chem. Int. Ed. 62 (2023) e202308194.
[31] X. Liu, S. Wang, W. Xie, et al., J. Mater. Chem. C 11 (2023) 7405–7410.
[32] J. Lu, J. Gao, W.F. Wang, et al., J. Mater. Chem. C 9 (2021) 5615–5620.
[33] R.G. Denning, J. Phys. Chem. A 111 (2007) 4125–4143.
[34] S.L. Hanna, O.K. Farha, Chem. Sci. 14 (2023) 4219–4229.
[35] A. Raghavan, C.L. Cahill, Angew. Chem. Int. Ed. 63 (2024) e202318161.
[36] Y. Wang, X. Yin, W. Liu, et al., Angew. Chem. Int. Ed. 57 (2018) 7883–7887.
[37] Y. Wang, Y. Wang, X. Dai, et al., Inorg. Chem. 58 (2019) 2807–2812.
[38] J. Ma, H. Lu, J. Yang, et al., Chin. J. Struc. Chem. 43 (2024) 100275.
[39] Y. Wang, X. Yin, J. Chen, et al., Chem. Eur. J. 26 (2019) 1900–1905.
[40] W. Liu, X. Dai, J. Xie, et al., ACS Appl. Mater. Interfaces 10 (2018) 4844–4850.
[41] Y. Zhang, X. Wang, K. Xu, et al., J. Am. Chem. Soc. 145 (2023) 13161–13168.
[42] H. Lu, Z. Zheng, J. Qiu, et al., Dalton Trans. 51 (2022) 3041–3045.
[43] H. Li, Y. Li, G. Qian, et al., Adv. Mater. 36 (2024) 2405535.
[44] H. Li, Q. Dong, G. Qian, et al., Adv. Funct. Mater. (2025) 2500445.
[45] H. Ding, M.J. Demkowicz, Acta Mater. 136 (2017) 415–424.
[46] B.N. Singh, J.H. Evans, A. Horsewell, P. Toft, G.V. Muller, J. Nucl. Mater. 258 (1998) 1908–1913.
[47] X. Song, Y. Wang, C. Wang, et al., J. Am. Chem. Soc. 146 (2023) 627–634.
[48] J. Wang, Y. Tu, X. Zhang, S. Guo, Polymer 289 (2023) 126485.
[49] W. Hu, L. Guo, L. Bai, Q. Fan, et al., Adv. Healthc. Mater. 7 (2018) 1800299.
[50] W. Liu, E. Song, L. Cheng, et al., Chem. Mater. 31 (2019) 9684–9690.